Mass transfer performance of modular catalytic structured packing
Proceedings of European Congress of Chemical Engineering (ECCE-6)
Copenhagen, 16-20 September, 2007

Mass transfer performance of modular catalytic structured packing

M. Behrens[a], Ž. Olujić[b], P.J. Jansens[b]

[a]*Air Products PLC, Hersham Place, Molesey Road, Walton on Thames, Hersham, Surrey KT12 4RZ, U.K.*
[b]*Delft University of Technology, Process & Energy Department, Separations Technology, Leeghwaterstraat 44, 2628 CA Delft, the Netherlands.*

Abstract

A mechanistic, parallel channel model was developed and validated experimentally to enable the prediction of mass transfer performance of the Katapak®-SP, a novel, modular catalytic structured packing. Total reflux distillation experiments were carried out at atmospheric pressure in a column with internal diameter of 0.45 m, using aqueous (Methanol/Water) and organic (Cyclohexane/n-Heptane) test systems. With the latter, two types of Katapak-SP were tested. In the pre-loading region of operation, the Katapak-SP12 packing exhibited with the aqueous system a constant and significantly better efficiency (HETP ~ 0.27 m) than with the organic system (HETP ~ 0.35 m). Under the same conditions, Katapak-SP11 appeared to be less efficient (HETP ~ 0.5 m). This is mainly due to a pronounced liquid maldistribution inside the closed flow channels, and best performance in both cases was reached upon onset of loading, when vapour phase forces liquid collected at transitions between packing layers to spread laterally. With both phases distributed evenly a peak in efficiency is achieved, and upon onset of flooding the efficiency starts to deteriorate strongly. The proposed Delft MCSP model, assuming plug flow of both phases, appeared to be too optimistic in the preloading region, but well capable of predicting the (best) mass transfer performance as observed around the loading point of the packed bed.

Keywords: reactive distillation, catalytic packing, Katapak-SP, mass transfer efficiency

1. Introduction

Catalytic distillation combines two processes, i.e. reaction with the aid of heterogeneous catalysis and thermal separation, in one unit operation. The majority of related publications focuses on the development of equilibrium and rigorous non-equilibrium

models to simulate the process [1]. However, little attention has been paid to hardware design and performance. For an accurate catalytic distillation column design the hydrodynamic and mass transfer performance imposed by the column internals is essential information. In order to be able to use such models for the design purposes, mass transfer behaviour and its dependence on liquid and vapour loads have to be known [2].

The combination of heterogeneous catalysis with separation requires the catalyst to be embedded in the column internal. Basically there are two possible options [3]. One is catalytic coating of packings or manufacturing the packing from catalytically active material. The other option is the immobilisation of catalyst in a part of the internal. Due to its bi-functional nature, an example of the latter is Modular Catalytic Structured Packings (MCSP). MCSP allows the adjustment of the catalyst volume and separation performance depending on process needs [4].

In catalytic distillation reaction is superimposed on separation by distillation. For slow reactions large residence times and therefore large hold-ups are necessary in the reactive stages, for fast reactions the internal should be selected based on its separation efficiency. The choice of equipment is principally determined by the reaction velocity and the relative volatility [1]. The latter determines the stage and reflux requirement. The intrinsic vapour-liquid separation capability of a type of catalytic internal is determined by its separation performance without reaction.

Limited data on the separation performance of catalytic packings is contained in literature. Information on the performance of three basic, but geometrically different catalytic structured packings can be found, including the Bale packing [5,6] where the catalyst particles are immobilised in a fibreglass cloth belt, the Katapak®-S [4,7,8] where the catalyst is immobilised between wire gauze sheets and the modular catalytic structured packing like Multipak® [9,10] and Katapak®-SP [4,11], where the catalyst containing pockets are separated by one or more corrugated sheets of a commercial structured packing.

According to Subawalla et al. [5] the mass transfer performance of the Bale packing increases with increased vapour load. Experimental evidence was obtained at 138 and 241 kPa with the test systems Cyclohexane/n-Heptane and Acetone/Methyl-Ethyl-Ketone at total reflux. The HETP ranges from 0.55 down to 0.3 m at the loading point. The proposed model assumes that the void space available for vapour flow is represented by a number of channels of characteristic dimension. The liquid in such a channel flows in the form of rivulets and drops, which are considered to contribute to the mass transfer. The mass transfer characteristics of this packing type are evaluated as a function of its main properties, the external surface area and amount of catalyst [6]. The mass transfer efficiency can be adjusted by varying the amount of fibreglass cloth used and the amount of catalyst inside the packing.

The vapour-liquid mass transfer efficiency of the Katapak-S is addressed in [4] and [7]. The test system was Chlorobenzene/Ethylbenzene at total reflux. The laboratory scale packing where the column diameter is 70 mm, has a HETP of 0.33 m while the industrial scale packing, column diameter of 200 mm, exhibited a lower separation efficiency (HETP ~ 1 m), which is caused mainly by the difference in installed specific surface area (270 vs. 85 m^2/m^3). Sherwood number type correlations fitted on experimental desorption (liquid side) and absorption (vapour side) data can be found in [8].

The Multipak and Katapak-SP are so called modular catalytic structured packing types. There are two versions of the Multipak. The difference is in the volume fraction of the catalyst and the type of corrugated sheet which is sandwiched between the catalyst containing pockets. Total reflux tests were done with the system Chlorobenzene/Ethylbenzene in a column with the internal diameter of 98 mm. As expected, the version with larger specific area exhibited higher separation efficiency, with an HETP ranging from 0.17 m at low column loads to 0.25 m in the loading range [9]. The other version has a HETP of 0.33 m [10].

The Multipak is an equivalent structure of the Katapak-SP11, i.e. both consist of catalyst pockets separated by one corrugated sheet of different design. For this packing the HETP, determined experimentally using Water/Acetic acid with medium water content at low column loads, was about 0.5 m [11]. According to Goetze et al. [4], Katapak-SP12 that contains two corrugated sheets inserted in between catalyst pockets, generates an average HETP of 0.4 m, which however was determined with the system Chlorobenzene/Ethylbenzene under total reflux conditions.

All published data were experimentally determined and used either directly or correlated in Sherwood relations as input value for the (non-)equilibrium models describing the catalytic process.

The objective of this study is to develop and validate experimentally at an appropriate scale a general parallel channel model capable of predicting the vapour-liquid mass transfer efficiency, taking into account the effects of variable geometry of Modular Catalytic Structured Packing (Katapak-SP) and system properties.

2. Model Development

2.1 MCSP Geometry

Figure 1 shows the two configurations of Katapak-SP, a commercially available MCSP evaluated in this study. Katapak-SP12 and Katapak-SP11 are shown on the left- and right hand side, respectively. In a MCSP, corrugated sheets are sandwiched between catalyst containing pockets. The latter is the reaction section of the packing with two pockets per layer height where the catalyst is contained in the packing. Due to the dense structure of these pockets gas is not able to penetrate into these pockets and cannot flow through this section. The space wherein the corrugated sheets are in the packing is the distillation section. In case of Katapak-SP12 the catalyst pockets are separated by two- and in case of Katapak-SP11 by one corrugated sheet. As it will be shown later on, this difference in the number of sheets fitted between the catalyst filled pockets affects significantly the hydraulic and mass transfer performance of a MCSP.

The corrugated sheets in this MCSP are of the MellapakPlus 752.Y type, which is an established high capacity packing (HCP) with corrugated sheets bended to the vertical at both ends of the flow channel. This geometry is beneficial and provides a smooth transition of the phases between packing layers leading to delayed loading and flooding effects in the packed bed. Furthermore the sheets are perforated, and some 10 per cent of the specific area is occupied by holes. In the Katapak-SP11 only one sheet alters with the catalyst filled pockets. Therefore in the distillation section only closed channels are present. It is assumed that traffic of the phases through the holes is negligible thus the

phases have to follow the flow channel to the end within a packing element height. In the Katapak-SP12 two sheets are placed between the catalyst filled pockets. Here in the middle of the distillation section the common crossing flow configuration is encountered as in a corrugated sheet structured packing. These channels are the open channels in this section of the MCSP. Since the corrugated sheets employed in Katapak-SP packings are of the MellaapakPlus 752.Y type, this packing has been included as reference in this study. The geometric features of two Katapak-SP packings and MellapakPlus 752.Y are given in Table 1.

2.2 Delft MCSP Model

Based on the geometry of MCSP, a parallel channel approach was adopted to predict the fluid dynamics and mass transfer behaviour of these packing types. As basis the Delft model [12-14], developed to predict the performance of corrugated sheet structured packing without using any empirical, packing type or size specific constants is used. The so called Delft MCSP Model makes a distinction between the three basic flow configurations, i.e. flow channel types that can be encountered in a MCSP: the catalyst filled pockets in the reaction section, and open and closed channels in the distillation section.

As illustrated schematically in Fig. 2, which shows the framework of the Delft Parallel Channel Model, the linking parameter is the liquid hold-up. Two contributions, i.e. internal and external hold-up determine the total hold-up. The internal hold-up is the amount of liquid inside the catalyst filled pockets. The maximum internal dynamic liquid hold-up, described in detail in [15], is reached at the catalytic load point, which is the point where the pockets are just full (saturated) with flowing liquid. At liquid loads above the catalytic load point the excess liquid contributes to the external hold-up, which is the liquid descending in the distillation section [16]. The excess liquid is assumed to be evenly distributed over the channels in the distillation section of the packing. This is ensured to some extent by the fact that the subsequent packing elements are rotated to each other by 90 degrees, and therefore between packing layers the space is available for the flowing fluids to mix and spread laterally, which tends to improve at increasing vapour loads. The static hold-up in the flow channels is omitted since it is relatively small and it has negligible influence on the mass transfer efficiency.

In the catalyst containing pockets only liquid will flow. The dense structure of the wire gauze pockets and catalyst bed prevents inside vapour flow. This means that the vapour-liquid mass transfer will take place only in the distillation section of the MCSP since here a vapour-liquid interface is available.

The open channels in the distillation section, which are the channels in the middle of this section of the packing, resemble the situation encountered in corrugated sheet structured packings. Therefore these channels will be treated equally as in the reference packing MellapakPlus 752.Y.

The closed channels are the channels next to the pockets. Both liquid and vapour are forced to follow the channel to the end. The liquid tends to flow in the form of rivulets along the lowest point of the channel. In this way a limited interface is available for contact with the ascending vapour. Regarding the fact that the corrugated sheets have a regular pattern of holes the extent of traffic of the phases through the holes is limited and

therefore not considered explicitly in the model. With respect to the geometry in case of the Katapak-SP11 only closed channels are present, while the Katapak-SP12 includes both closed and open channels.

The Delft MCSP model is a mechanistic, parallel channel model. To make a distinction between the two configurations, two relevant, geometry based ratios are defined, i.e. the cross sectional ratio and the open channel ratio, respectively:

To make a distinction between the two configurations, two relevant geometric based ratios are defined, the cross sectional ratio and the open channel ratio, respectively:

$$\Gamma = \frac{\text{cross sectional area occupied by the corrugated sheets}}{\text{total cross sectional area column}} \qquad \text{Eq. 1}$$

$$X = \frac{\text{number o fopen channels in the distillation section of MCSP}}{\text{total number of channels in the distillation section}} \qquad \text{Eq. 2}$$

Each channel has its contribution to the mass transfer process and the overall calculation procedure is shown in Figure 3. It is assumed that the flowing phases are able to fully mix at the transition between packing layers and this lateral mixing is promoted especially at higher F-factors. This consequently means that between packing layers the concentrations in both phases are uniform over the column cross section.

Packed columns are continuous differential contacting devices however the HETP is preferred to characterise the mass transfer efficiency. The HETP is related to the HTU's, i.e. the phase velocities and volumetric mass transfer coefficients, via the stripping factor, λ, which is the ratio of slopes of the equilibrium and operating lines. The change in composition is calculated based on the height of transfer units, $HTU_{L,cc}$, $HTU_{G,cc}$, $HTU_{L,oc}$ and $HTU_{G,oc}$, the corresponding HETP's and using the Fenske equation where the mole fraction at the end of the channel is written explicitly, all based on the geometry of respectively closed and open channels. At the transition between layers the average composition is calculated by mixing of the flows according the flow contribution in each channel, i.e. taking the cross sectional and channel ratio into account. In catalyst filled pockets liquid must flow out of the upper pockets before it can enter the lower pockets and in between it mixes with the liquid flowing in the closed channel. This is taken into account in the model by intermediate mixing of liquid coming from both channels before it is redistributed.

Based on the average concentration entering and leaving a packing layer the average number of equilibrium stages per packing layer height, $N_{min,i}$, is determined using the Fenske equation.

$$N_{\min,i} = \frac{\ln\left(\frac{x_{in,i}}{1-x_{in,i}}\frac{1-x_{av,i}}{x_{av,i}}\right)}{\ln(\alpha_i)} \qquad (3)$$

where $x_{in,i}$ is the mole fraction of more volatile (light key) component entering a packing layer, $x_{av,i}$ is the average composition leaving the packing layer, and α_i is the relative volatility in the packing layer calculated with the composition entering the packing layer.

The relative volatilities as function of the composition for two test systems were taken

from [18]. The relative volatility over a packing layer height is taken constant, and this value is used to estimate the corresponding value of the stripping factor:

$$\lambda = m = \frac{\alpha_i}{\left[1 + (\alpha_i - 1) x_{lk}\right]^2} \tag{4}$$

where x_{lk} is the mole fraction of the light key, i.e. $x_{in,i}$. It should be noted that under total reflux conditions, the stripping factor is equal to the slope of the equilibrium line, m.

This is repeated for the number of MCSP layers, n_{pe}, contained in the installed bed. The HETP is determined with the height of the packed bed divided by the total number of stages in the column, which is the sum of the number of stages in each packing layer:

$$HETP = \frac{n_{pe} h_{pe}}{\sum_{n_{pe}} N_{\min,i}} \tag{5}$$

2.1.1 Working equations

The open channels are similar to the flow channels in the HCP where the description of the mass transfer is based on the high capacity geometry with crossing flow channels.
The HETP in the open channels as used in the algorithm is calculated with:

$$HETP_{oc} = \left[\frac{\ln \lambda_i}{\lambda_i - 1}\right] HTU_{Go,oc,i} \tag{6}$$

where the $HTU_{Go,oc,i}$ is the overall gas phase height of transfer unit in the corresponding packing layer which is defined as:

$$HTU_{Go,oc,i} = HTU_{G,oc,i} + \lambda_i HTU_{L,oc,i} \tag{7}$$

where $HTU_{G,oc,i}$ and $HTU_{L,oc,i}$ are respectively the gas and liquid side height of transfer unit in the element.

The local height of transfer unit for vapour and liquid phase, respectively, in these channels is defined as:

$$HTU_{G,oc} = \frac{u_{G,D}}{k_{G,oc} a_{e,oc}} \tag{8}$$

and

$$HTU_{L,oc} = \frac{u_{L,D}}{k_{L,oc} a_{e,oc}} \tag{9}$$

where $u_{G,D}$ is the gas velocity in the distillation section of the packing, $k_{G,oc}$ is the gas phase mass transfer coefficient, $a_{e,oc}$ the effective (interfacial) area, $u_{L,D}$ the liquid velocity in the distillation section which takes into account the excess liquid in this section above the catalytic load point [12], and $k_{L,oc}$ is the liquid phase mass transfer coefficient.

The column cross sectional area for the gas is reduced because of the catalyst filled pockets in the MCSP, thus the gas velocity in the distillation section is defined as:

$$u_{G,D} = \frac{u_{Gs}}{\Gamma} \tag{10}$$

where u_{Gs} is the superficial vapour (gas) velocity.

Since in the distillation section of the packing two types of flow channels are identified and these differ in geometry, in the geometry based Delft MCSP model the mass transfer in the channels is described accordingly. Thus each channel in the model exhibits its own separation performance due to the geometry imposed hydrodynamics.

Mass transfer coefficients

The mass transfer results from the vapour-liquid interaction at the interface, i.e. film surface, along relatively short flow channels and accompanied with considerable entrance effects. To account properly for this the vapour phase mass transfer coefficient incorporates the effective relative velocity based Reynolds number, the vapour phase Schmidt number, the vapour-liquid friction factor and the characteristic flow channel diameter to length ratio.

In the vapour phase to account for the flow regime transition, the vapour phase mass transfer coefficient, k_G, has a laminar and turbulent contribution:

$$k_{G,oc} = \sqrt{k_{G,lam,oc}^2 + k_{G,turb,oc}^2} \tag{11}$$

The laminar flow contribution is determined with:

$$k_{G,lam,oc} = \frac{Sh_{G,lam,oc} D_G}{d_{hG}} \tag{12}$$

where $Sh_{G,lam}$ is the laminar flow regime Sherwood number and D_G is the gas phase diffusion coefficient. The gas hydraulic diameter is defined as:

$$d_{hG} = \frac{\frac{(bh - 2\delta s)^2}{bh}}{\left[\left(\frac{(bh - 2\delta s)}{2h}\right)^2 + \left(\frac{(bh - 2\delta s)}{b}\right)^2\right]^{0.5} + \frac{bh - 2\delta s}{2h}} \tag{13}$$

where b is the corrugation base width, h is the corrugation height, s is the corrugation side length and δ is the liquid film thickness in the channels which can be found in [16].
The laminar flow regime Sherwood number is defined as:

$$Sh_{G,lam,oc} = 0.664 Sc_G^{1/3} \sqrt{\mathrm{Re}_{Grv,oc} \frac{d_{hG}}{l_{G,pe}}} \tag{14}$$

where Sc_G is the vapour phase Schmidt number, Re_{Grv} is the relative effective velocity based Reynolds number and $l_{G,pe}$ is the length of the gas flow channel in a packing element. These dimensionless numbers are respectively defined as:

$$Sc_G = \frac{\mu_G}{\rho_G D_G} \tag{15}$$

where μ_G is the gas phase dynamic viscosity and ρ_G is the gas density,

$$\mathrm{Re}_{Grv,oc} = \frac{\rho_G \left(u_{Ge,oc} + u_{Le,oc}\right) d_{hG}}{\mu_G} \tag{16}$$

where $u_{Ge,oc}$ and $u_{Le,oc}$ are respectively the effective gas and liquid velocities in these channels. The effective gas velocities have to be determined iteratively since the different channels have a different geometry and therefore the gas experiences different resistances

for flow, this is described in [17]. The effective liquid velocity is defined as:

$$u_{Le,oc} = \frac{u_{L,D}}{\varepsilon_D h_{L,oc} \sin(a_L)} \tag{17}$$

where ε_D is the porosity of the distillation section in the MCSP, which is equal to that of the HCP, $h_{L,oc}$ is the dynamic liquid hold-up in the open channels, described thoroughly elsewhere [12], and α_L is the effective liquid flow angle. The latter is defined based on the geometry of V-shaped gas flow channel as

$$a_L = \arctan\left[\frac{\cos(90 - a_c)}{\sin(90 - a_c)\cos\left(\arctan\left(\frac{b}{2h}\right)\right)}\right] \tag{18}$$

The length of the gas flow channel in a packing layer is determined with:

$$l_{G,pe} = \frac{h_{pe} - h_{vertical}}{\sin a_c} + h_{vertical} \tag{19}$$

where h_{pe} is the height of a packing layer, $h_{vertical}$ is the height of the vertical part of the high capacity flow channel and α_c is the corrugation inclination angle with respect to the horizontal in the middle of the channel. The values for the HCP as part of the distillation section in the MCSP are respectively $h_{vertical} = 20$ mm and $\alpha_c = 41°$.

The turbulent gas phase mass transfer coefficient is determined with the corresponding turbulent flow regime Sherwood number:

$$k_{G,turb,oc} = \frac{Sh_{G,turb,oc} D_G}{d_{hG}} \tag{20}$$

with

$$Sh_{G,turb,oc} = \frac{\mathrm{Re}_{Grv,oc}\, Sc_G \frac{\xi_{GL,oc}\varphi_{oc}}{8}}{1 + 12.7\sqrt{\frac{\xi_{GL,oc}\varphi_{oc}}{8}}\left(Sc_G^{2/3} - 1\right)}\left(1 + \left(\frac{d_{hG}}{l_{G,pe}}\right)^{2/3}\right) \tag{21}$$

where $\xi_{GL,oc}$ is the gas-liquid friction factor which contributes to the mass transfer and φ_{oc} is the fraction of the flow channel occupied by the liquid. The latter is defined as:

$$\varphi_{oc} = \frac{2s}{b + 2s} \tag{22}$$

The gas-liquid friction factor is calculated with:

$$\xi_{GL,oc} = \left(-2\log\left(\frac{\delta_{oc}/d_{hG}}{3.7} - \frac{5.02}{\mathrm{Re}_{Grv,oc}}\log\left(\frac{\delta_{oc}/d_{hG}}{3.7} + \frac{14.5}{\mathrm{Re}_{Grv,oc}}\right)\right)\right)^{-2} \tag{23}$$

The liquid phase mass transfer coefficient is based on the penetration theory of Higbie where the contact, i.e. exposure time in the laminar film is defined with the characteristic length and effective liquid velocity:

$$k_{L,oc} = 2\sqrt{\frac{D_L u_{Le,oc}}{0.9\pi d_{hG}}} \tag{24}$$

where D_L is the liquid side diffusion coefficient.

Effective interfacial area

The effective interfacial area is determined using well known Onda correlation adapted to corrugated sheet structured packing [15]. In the Delft parallel channel model the effective mass transfer area in the open channels is calculated with:

$$a_{e,oc} = (1-\Omega)\, a_{e,Onda,oc} \tag{25}$$

where Ω is the (void) fraction of specific geometric area occupied by perforations in the sheets and $a_{e,Onda,oc}$ the effective area prediction based on the Onda equation:

$$a_{e,Onda,oc} = \frac{a_{p,oc}}{\Gamma X}\left\{1 - \exp\left[-1.45\left(\frac{0.075}{\sigma_L}\right)^{0.75} \mathrm{Re}_{Ls,oc}^{0.1}\, Fr_{Ls,oc}^{-0.05} We_{Ls,oc}^{0.2}\right]\right\} \tag{26}$$

where $a_{p,oc}$ is the specific area installed in the open channels of the MCSP, σ_L is the liquid surface tension, $Re_{Ls,oc}$ is the liquid Reynolds number in the open channels, $Fr_{Ls,oc}$ is the Froude number and $We_{Ls,oc}$ the corresponding Weber number. These dimensionless numbers are used in conjunction with the cross sectional and channel ratios defined by Eqs (1) and (2), respectively, to account for the installed area per unit volume occupied by open channels in the parallel channel model to calculate the effective area per unit volume of these channels, i.e. the local effective area:

$$\mathrm{Re}_{Ls,oc} = \frac{\Gamma X \rho_L u_{Ls,D}}{a_{p,oc}\mu_L} \tag{27}$$

$$We_{Ls,oc} = \frac{\Gamma X \rho_L u_{Ls,D}^2}{a_{p,oc}\sigma_L} \tag{28}$$

$$Fr_{Ls,oc} = \frac{a_{p,oc} u_{Ls,D}^2}{\Gamma X g \sin(\alpha_L)} \tag{29}$$

where ρ_L is the liquid density, μ_L the liquid dynamic viscosity, and g the is gravitational acceleration.

The closed channels are the flow channels next to the catalyst filled pockets. Of course similar relations for mass transfer apply as developed for the open channels, however here as a function of the closed channel geometry. Since two pockets above one another are present in the reactive section of the MCSP all liquid flowing out of the upper pocket is able to mix with the liquid flowing in this channel, which, as mentioned before, is accounted for in the modelling.

The vapour phase mass transfer coefficient is determined using the same equations however based on the closed channel geometry. The difference in gas hydraulic diameter in both channels is negligible so these are taken equal. In the Sherwood relations the relative velocity based Reynolds number in these channels is defined with the effective velocities encountered here. The effective vapour velocity follows from the study on the

pressure drop and capacity of MCSP [17] and the effective liquid velocity is defined with the dynamic liquid hold-up, $h_{L,cc}$, and is determined based on the liquid film thickness and the specific area, which is elaborated in detail elsewhere [16]. It should be noted that the model, in case of the turbulent flow regime, for closed channels assumes that all three channel sides are wetted ($\varphi_{cc} = 1$).

The effective mass transfer area is determined with Eq. (25), based on the geometry of the closed channels, and therefore in the Onda equation, $a_{p,cc}$ is divided by $\Gamma(1 - X)$ to determine the local effective area per unit volume occupied by these channels for correct use in the parallel channel model.

3. Experimental Studies

The mass transfer performance was experimentally determined using a pilot scale, 450 mm internal diameter, total reflux distillation column. The setup is described in detail in [19] and a simple flow diagram is shown in Figure 3. The column, constructed of stainless steel, is about 4 metres in height in which a packed bed can be installed up to 2.5 m. The reflux flow was measured accurately using a coreolis type mass flow meter. Based on these flows the average F-factor in the column was determined taking into account the effect of reflux subcooling. At each start-up the installed packed bed was flooded for some time to ensure thorough wetting of the packing. Then the column load was set to the desired value and the system was given time to stabilise (constant temperature and pressure profiles). After stabilisation of the system, three samples of the liquid flowing out of the packed bed and the reflux were taken every 30 minutes.

The total reflux distillation experiments were done with two systems, Methanol/Water (MeOH/Wa) and Cyclohexane/n-Heptane (CH/nH). The first system was chosen because a set of MCSP-12 was filled with a catalyst in an aqueous environment. Since the other MCSP's were filled with glass beads the CH/nH system was chosen since this is the principal test system for compatibility reasons. The samples of the aqueous system were analysed by means of Karl-Fisher coulometric titration and the organic system samples were analysed using a gas chromatograph.

Also the pressure drop over the column was determined as function of gas load with two calibrated pressure difference meters, a low range one from 0 to 10 mbar and one full range for 0 to 100 mbar. An overview of the experiments done is given in Table 2. A summary of characteristic average physical properties is given in Table 3.

4. Results and Discussion

Figure 5 shows the efficiency curves of the reference high capacity packing (HCP) as a function of F-factor, as observed with respectively aqueous and organic systems [19]. The CH/nH system has a constant HETP up to flooding where the efficiency, upon reaching the point of onset of flooding suddenly disappears. The better efficiency with the MeOH/Wa system, which is pronounced in the preloading region, can be attributed mainly to the effect of the rather short bed used compared to that with the CH/nH system where a good initial distribution is preserved within the first 5 to 6 elements only. Also,

with MeOH/Wa system the loading region is wider, wherein the efficiency gradually deteriorates since more effort is needed to entrain liquid due to the higher surface tension of this system. At higher F-factors this deterioration is more pronounced and HETP values reach that observed with the Ch/nH system.

Figure 6 shows the experimental HETP's as a function of F-factor obtained with the MCSP with the different systems. For the MCSP-12 with the aqueous system the efficiency in the pre-loading region is about constant. At loading, where the contact between the phases is more intensive a somewhat lower HETP is observed before the bed is flooded (sharp increase of the HETP). The void fraction in the MCSP at the transition between packing layers is somewhat larger than along the pockets of the reaction section, and at loading point, the liquid starts to accumulate in this space where it is thoroughly mixed and spread laterally resulting in an intensified contact between the phases that is beneficial to the mass transfer process. Approaching the flooding, the axial dispersion, i.e. backmixing of liquid in the packed bed increases to the extent that causes the mass transfer efficiency to deteriorate and disappear eventually.

Where with the aqueous system the separation performance is nearly constant in the pre-loading region, with the organic system the HETP is substantially higher. The difference in behaviour between the systems is mainly determined by the difference in liquid surface tension. Due to the higher liquid surface tension of the aqueous system the liquid film developed over the installed packing surface is more stable. Therefore a higher vapour-liquid interaction is possible without film break-up. Certainly this will also help with reaching higher capacities but the higher capacity with the aqueous system is mainly caused by an about twice as low liquid load at the same F-factor (see Table 3). The catalyst filled pockets are made of wire gauze metal to immobilise the particles in the MCSP and to ensure liquid access. The difference in experimental results between the systems indicates that the liquid spreads better over the outside surface of the pockets with the aqueous system because of higher capillary forces due to the liquid surface tension providing a liquid film contributing to mass transfer.

The HETP's of the MCSP's are higher compared to the HCP. This is not surprising regarding the specific geometric area of both versions of the MCSP is much lower than that of the HCP. However, the deteriorating effect on HETP is enhanced due to a reduced possibility of radial spreading in the MCSP because of the catalyst filled pockets. This behaviour that appeared pronouncedly detrimental to the performance of the MCSP-11 has been observed earlier [20]. In the packed bed with MCSP-11 all available flow channels in the distillation section of the packing are closed channels. Although the installed geometric specific area of MCSP-11 is somewhat lower than that of MCSP-12 (MCSP-11 : MCSP-12 = 300.2 : 341.3 m^2/m^3), the poor efficiency in the pre-loading region is mainly attributed to the liquid maldistribution effect. The reason of this maldistribution is twofold, liquid bypassing through the catalyst filled pockets and because of the closed channel structure initial liquid distribution feeds only a few channels with liquid. This means that a considerable part of the channels are not active in the mass transfer process. Also there is a channelling effect within these channels, i.e. the liquid flows preferably at the lowest point leaving part of the channel "dry". The presence of the pockets between the corrugated sheets avoids this lateral spreading of the liquid within a packing layer. The mixing of liquid at the crossings of corrugated sheets, as present in the HCP and partly present in the MCSP-12, is absent. Thus the liquid

maldistribution tends to propagate downwards in the packed bed. The lateral spreading in the MCSP-12 packed bed is better since part of the channel in the distillation section has an equal structure as in the reference HCP (open channel geometry) which results in a more efficient mass transfer process. The improvement of the mass transfer beyond loading point is pronounced because of enhanced lateral spreading at the transition between packing layers. Again the best performance is experienced during hydraulic loading of the packed beds.

The Delft parallel channel model is used specifically to predict the performance of the MCSP. The system physical properties taken for the model calculations are summarised in Table 3. In Figure 7 the results of the MCSP model is compared with the MCSP-12 with the system MeOH/Wa. Compared to the HCP the MCSP has less installed specific geometric area and due to the MCSP geometry liquid bypasses the vapour while flowing through the catalyst filled pockets, which additionally lowers the mass transfer and this is incorporated in the model. Up to flooding the model is well capable to predict the efficiency, since flooding phenomena still are not fully understood and cannot be accurately predicted, these effects are not incorporated in the model.

The model calculations with the organic CH/nH system are compared in Figure 8 and 9 for respectively the MCSP-12 and MCSP-11. Since the model assumes uniform distribution of the phases over the column cross section, at each column load the model prediction is therefore too optimistic in the pre-loading region. Regarding the fact of the outside surface area of the pockets in the closed channels participate in mass transfer, line 'a' in Figure 8 is the result of the model calculations of the MCSP-12 with the organic system where this outside area of the pockets is omitted as installed geometric area and therefore not contributing to the calculated effective interfacial area. As can be seen the model and experimental results are about on the same plateau in the pre-loading region indicating that this area is not optimally used in the MCSP.

The parallel channel (Delft MCSP) model predicts an equal HETP for both MCSP types. Because in the description of the vapour phase mass transfer coefficient is assumed that the complete channel is occupied by liquid, $\varphi_{cc} = 1$, this leads to a higher mass transfer coefficient in this channel and in the model the closed channel geometry is more beneficial for mass transfer and compensates for the less installed geometric area. Around loading the model agrees with the experiments.

The Delft MCSP model predicts an about equal efficiency with the organic system and the aqueous system. The model prediction with the MeOH-Water system incorporate poorer wettability because of a higher surface tension, which in the model results in a much lower effective interfacial area prediction of roughly 120-135 m^2/m^3 (average 50%) compared to the organic system. However the difference in HETP prediction between the systems is much smaller then based on the effective area difference because the vapour side mass transfer resistance in the aqueous system is much lower since the vapour diffusivity is about 8 times higher and mainly compensates for the loss in effective area.

The most efficient mass transfer is reached at hydraulic loading where model predictions agree with experiments. It should be noted that according to the model prediction, the catalytic load points for two test systems, shown in Table 4 with corresponding F-factors, are well beyond the normal operating region since hydraulic loadings of the packed beds occur at a lower F-factor. This suggests that under proper hydraulic conditions the catalyst may not be fully wetted, i.e. reaction carried out with

less efficiency than expected. This is a point of concern when integrating reaction with separation.

The experimental results obtained in this study are comparable with data published in previous studies. For the MCSP-11 a HETP around 0.5 m at low column loads is found and this is also reported in [11] with an aqueous system. This indicates here that the geometry imposed flow behaviour of the MCSP mainly determines the efficiency. The performance with the organic system of the MCSP-12 with the reported data in [4] shows that the performance in this study with CH/nH are comparable. The same trend is observed while the column load approaches hydraulic loading of the bed where the separation efficiency increases rapidly. The experimental results obtained in this study are more difficult to compare with the Multipak since the corrugated sheets in the distillation section are different (wire gauze metal sheets as encountered in Montz A3-500 with a corrugation angle of 60^0) and the published data are results from tests in a column with a considerable smaller diameter where wall effects play an important role. The trend of the data obtained in this study is different then shown in [9] and is most probably due to the better wettability of the wire gauze sheets used in the Multipak.

5. Conclusions

The Delft MCSP model was developed to predict the mass transfer efficiency of Modular Catalytic Structured Packings. The model was validated using the results of total reflux distillation experiments carried out with two different test systems and two types of MCSP.

For the MCSP-12 the efficiency with the aqueous system is rather constant up to flooding. Here the model indicates that at the outside surface of the pockets a liquid film is developed due to high capillary forces which promote liquid spreading over the wire gauze metal surface. With the organic system higher HETP's are experimentally obtained and these values agree with model calculations where the wire gauze surface (outside surface of the pockets) is omitted from the effective interfacial area calculation.

The poorer performance the MCSP-12 and more pronouncedly MCSP-11 in the preloading region is caused by liquid maldistribution within closed channels leading to the poor wetting of channel walls. The assumption of uniform liquid distribution in the pre-loading region and consequently the interfacial area generation with the organic system gives too optimistic model predictions, which however match the best performance as observed in loading region.

The Delft MCSP model is well capable of predicting with good accuracy the mass transfer efficiency obtained with MCSP under operating conditions of practical interest.

Acknowledgements

The authors wish to thank Sulzer Chemtech for making available the Katapak® and Mellapak® packings as well as for the permission to publish the results. The authors also wish to thank the following M.Sc. students for their involvement and work, E.M. Brouwer, F.J. van Dijk en S. Balkenende.

Symbols

h_L	[-]	liquid hold-up
a	[m^2/m^3]	specific area
b	[m]	corrugation base
d	[m]	diameter
D	[m^2/s]	diffusion coefficient
Fr	[-]	Froude number
g	[m/s^2]	gravitational acceleration
h	[m]	height/corrugation height
HETP	[m]	height equivalent to a theoretical plate
HTU	[m]	height of transfer unit
k	[m/s]	mass transfer coefficient
l	[m]	length
m	[-]	slope of equilibrium line
Re	[-]	Reynolds number
s	[m]	corrugation side
Sc	[-]	Schmidt number
u	[m/s]	velocity
We	[-]	Weber number
x	[-]	mole fraction

Greek letters

α	[º]	corrugation angle with respect to the horizontal
α	[-]	relative volatility
X	[-]	open channel ratio
ξ	[-]	friction factor
δ	[m]	film thickness
Γ	[-]	cross sectional ratio
ε	[-]	void fraction
λ	[-]	stripping factor
ρ	[kg/m^2]	density
σ	[N/m]	surface tension
μ	[Pa·s]	dynamic viscosity
φ	[-]	V-shaped fraction of the channel occupied by liquid
Ω	[-]	fraction of holes in corrugated sheets

Subscripts

c	corrugation
cc	closed channel
D	distillation section
e	effective
G	gas
Ge	gas, effective
GL	gas-liquid
Gs	gas, superficial
h	hydraulic

hG	hydraulic gas
L	liquid
Le	liquid, effective
Ls	liquid, superficial
oc	open channel
p	packing
pe	packing element

Abbreviations

CH	cyclohexane
HCP	high capacity packing
MCSP	modular catalytic structured packing
MeOH	methanol
nH	normal heptane
Wa	water

References

[1] Sundmacher, K., Kienle, A., Reactive distillation, Status and future directions, Wiley-VCH (2003).
[2] Hoffmann, A., Noeres, C., Górak, A., Scale-up of reactive distillation columns with catalytic packings, (2004) *Chem. Eng. Proc*., 43, 383-395.
[3] Klöker, M., Kenig, E.Y., Górak, A., Markusse, A.P., Kwant, G., Moritz, P., Investigation of different column configurations for the ethyl acetate synthesis via reactive distillation, (2004) *Chem. Eng. Proc*., 43, 791-801.
[4] Götze, L., Bailer, O., Moritz, P., Scala, C. von, Reactive distillation with Katapak®, (2001) *Catal. Today*, 69, 201-208.
[5] Subawalla, H., González, J.C., Seibert, A.F., Fair, J.R., Capacity and efficiency of reactive distillation Bale packing: Modeling and experimental validation, (1997) *Ind. Eng. Chem. Res.*, 36, 3821-3832.
[6] Manduca, E., Gonzalez, J.C., Elman, H., Mass transfer characteristics of Bale-type catalytic distillation packings, (2003) *Sep. Sci. Technol*., 38, 14, 3535-3552.
[7] Moritz, P., Hasse, H., Fluid dynamics in reactive distillation packing Katapak®-S, (2004) *Chem. Eng. Sci*., 54, 1367-1374.
[8] Kolodziej, A., Jaroszyński, M., Bylica, I., Mass transfer and hydraulics for Katapak-S, (2004) *Chem. Eng. Proc*., 43, 457-464.
[9] Górak, A., Hoffmann, A., Catalytic distillation in structured packings: Methyl acetate synthesis, (2001) *AIChE J*. 47, 5, 1067-1076.
[10] Kolodziej, A., Jaroszynski, M., Salacki, W., Orlikowski, W., Fraczek, K., Klöker, M., Kenig, E.Y., Górak, A., Catalytic distillation for TAME synthesis with structured catalytic packings, (2004) *Chem. Eng. Res. Des*., 82(A2), 175-184.
[11] Steinigeweg, S., Gmehling, J., Esterification of a fatty acid by reactive distillation, (2003) *Ind. Eng. Chem. Res*., 42, 15, 3612-1619.
[12] Olujić, Ž., Behrens, M., Colli, L., Paglianti, A., Predicting the efficiency of

corrugated sheet structured packings with large specific surface area, (2004) *Chem. Biochem. Eng. Q.*, 18, 2, 89-96.
[13] Olujić, Ž., Development of a complete simulation model for predicting the hydraulic and separation performance of distillation columns equipped with structured packing, (1997) *Chem. Biochem. Eng. Q*. 11, 1, 31-46.
[14] Fair, J.R., Seibert, A.F., Behrens, M., Saraber, P.P., Olujić, Ž., Structured packing performance – Experimental evaluation of two predictive models, (2000) *Ind. Eng. Chem. Res.*, 39, 6, 1788-1796.
[15] Behrens, M, Liquid hold-up in catalyst containing pockets of modular catalytic structured packing, Chapter 3 in Hydrodynamics and Mass Transfer Performance of Modular Catalytic Structured Packing, *Thesis*, TU Delft, 2006.
[16] Behrens, M., Dynamic liquid hold-up in modular catalytic structured packing, Chapter 5 in Hydrodynamics and Mass Transfer Performance of Modular Catalytic Structured Packing, *Thesis*, TU Delft, 2006.
[17] Behrens, M., Pressure drop and capacity in modular catalytic structured packing, Chapter 6 in Hydrodynamics and Mass Transfer Performance of Modular Catalytic Structured Packing, *Thesis*, TU Delft, 2006.
[18] Onken U., Arlt, W., Recommended test mixtures for distillation columns, second edition, The Institution of Chemical Engineers, Rugby, U.K. (1990).
[19] Olujić, Ž., Behrens M., Spiegel, L., Modelling and experimental characterisation of the performance of a large specific area, high capacity structured packing, (2007) *Ind. Eng. Chem. Res*. 46, 883-893.
[20] Behrens, M., Saraber, P.P., Jansen, H., Olujić, Ž., Performance characteristics of a monolith-like structured packing, (2001) *Chem. Biochem. Eng. Q*., 15, 2, 49-57.

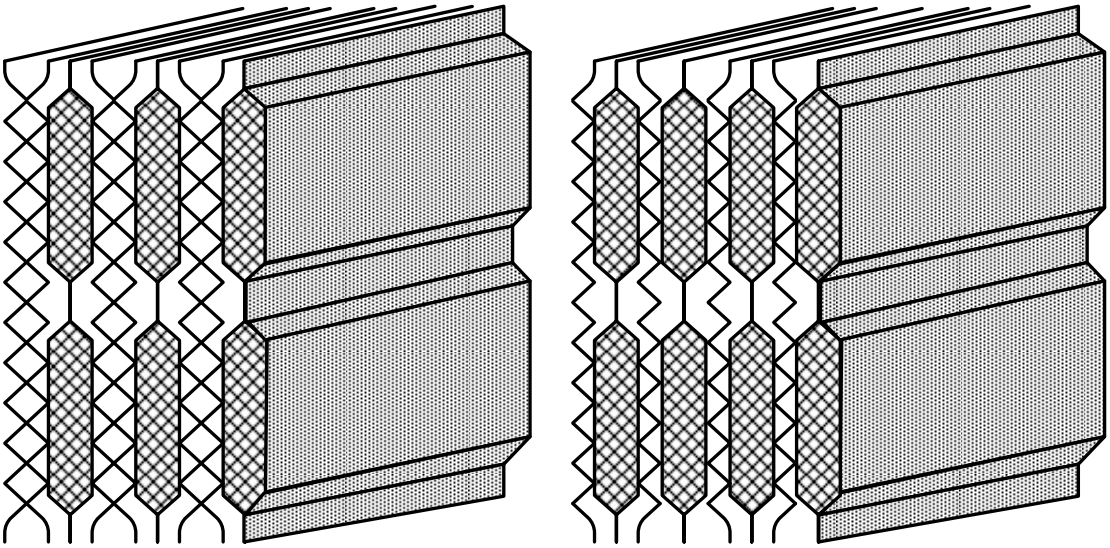

Figure 1 Schematic of modular catalytic structured packings (MCSP) considered in this study, left: MCSP-12; right MCSP-11

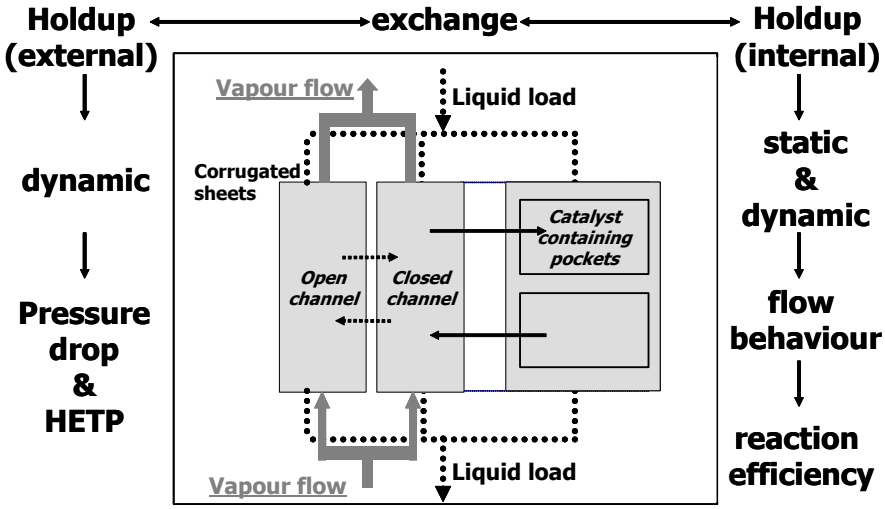

Figure 2 Delft MCSP Model framework

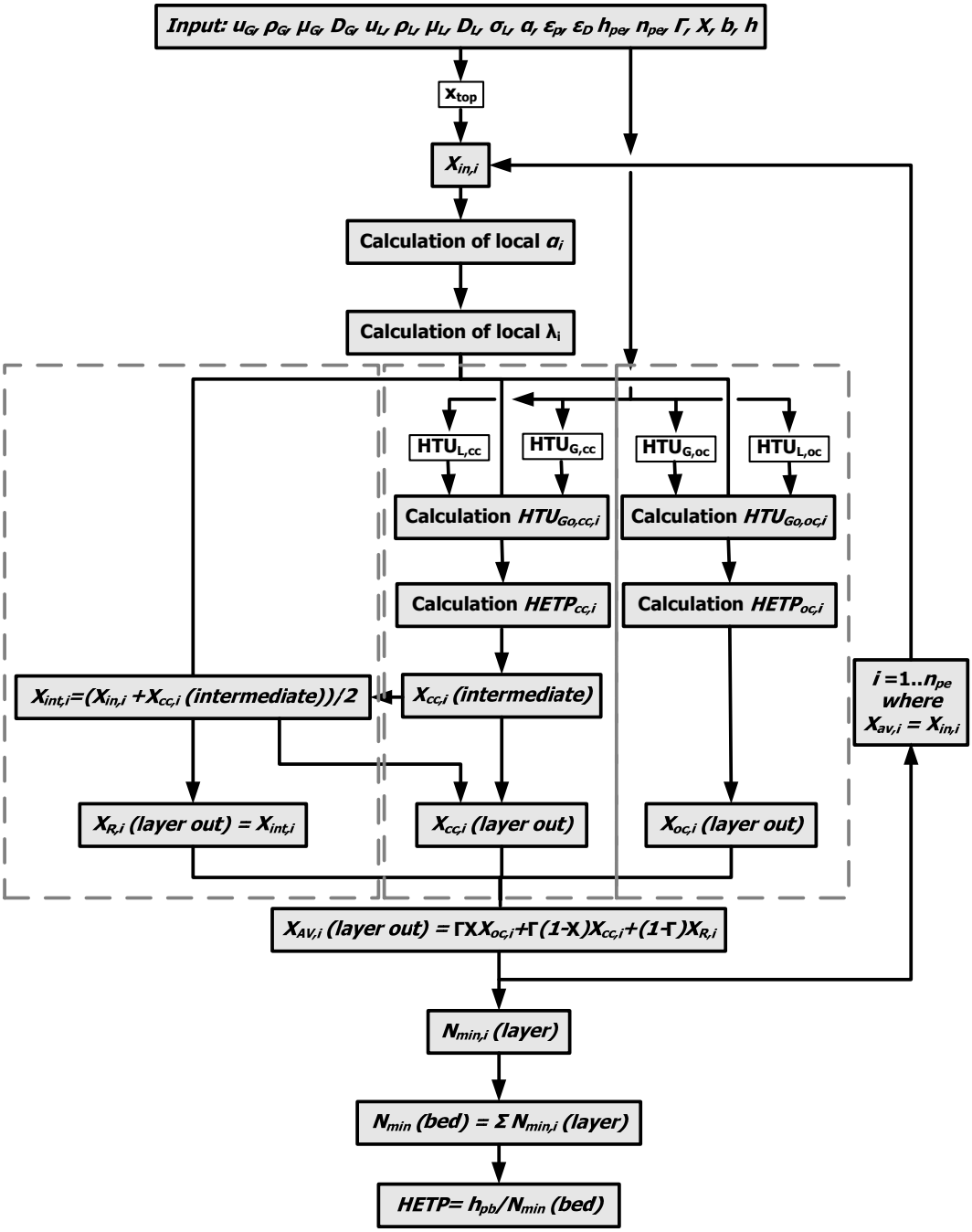

Figure 3 Algorithm for the calculation of the HETP of MCSP

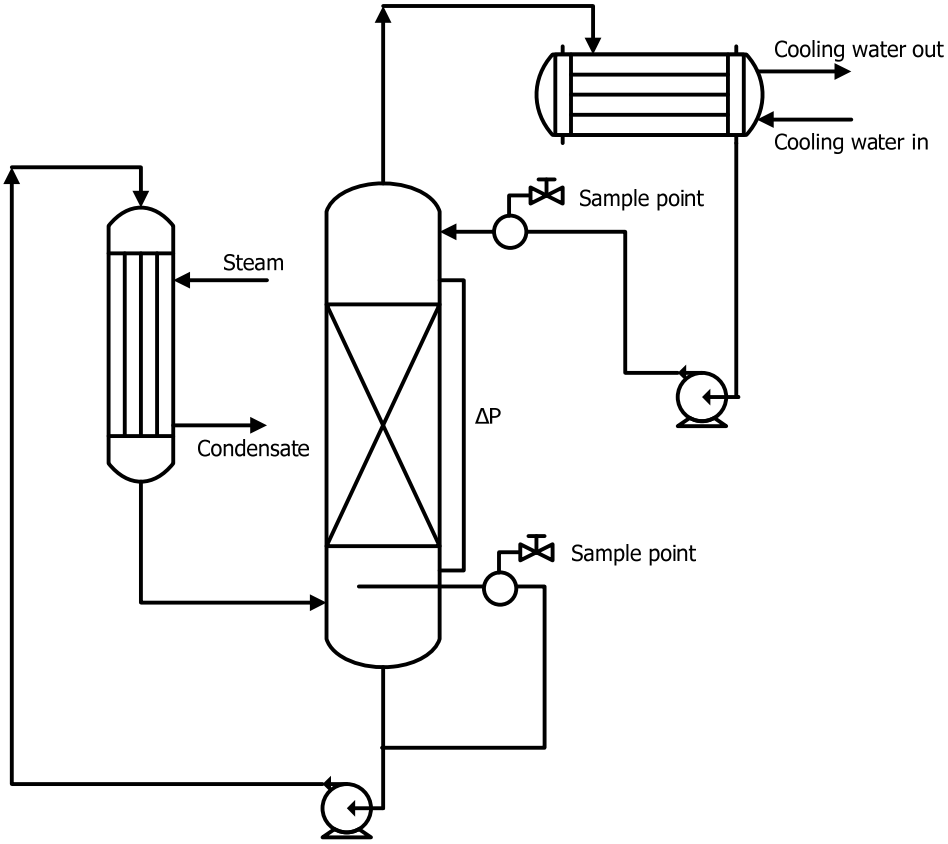

Figure 4 Schematic of TU Delft total reflux distillation column

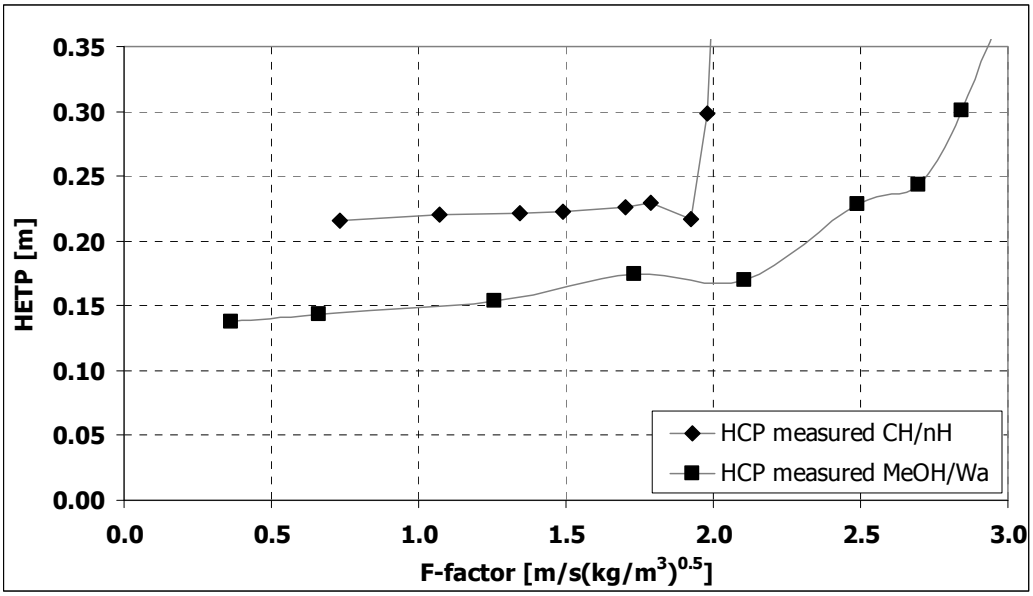

Figure 5 Efficiency (HETP) of the high capacity structured packing (HCP) as a function of F-factor as observed with methanol/water and cyclohexane/n-heptane systems, respectively, at atmospheric pressure.

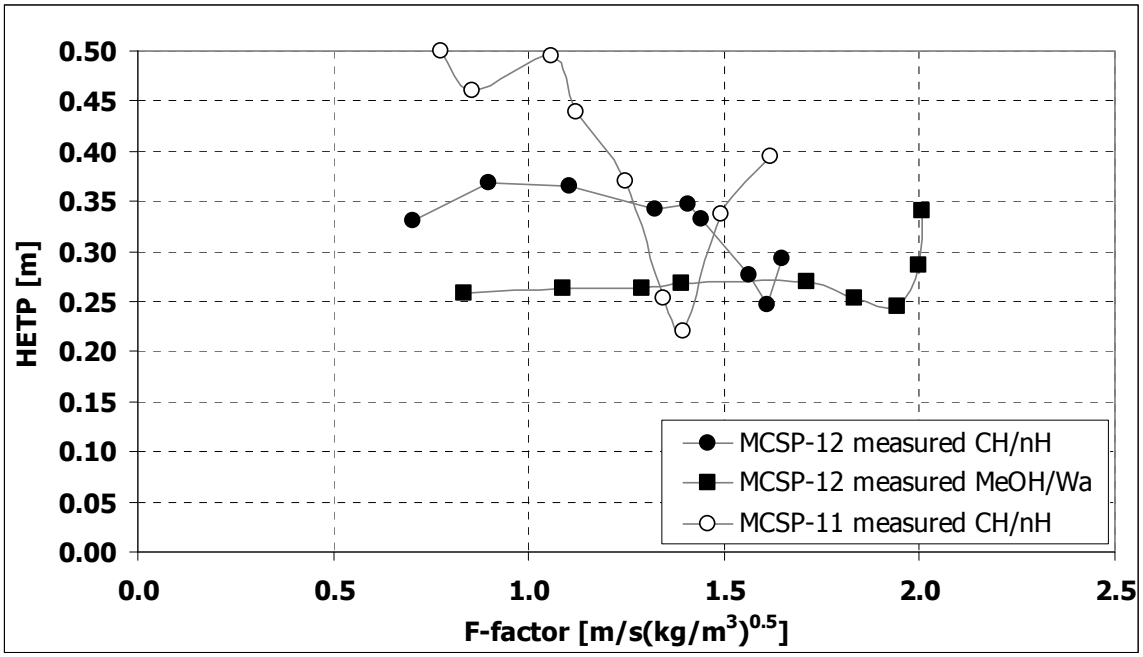

Figure 6 Measured HETP as a function of F-factor for two MCSP's.

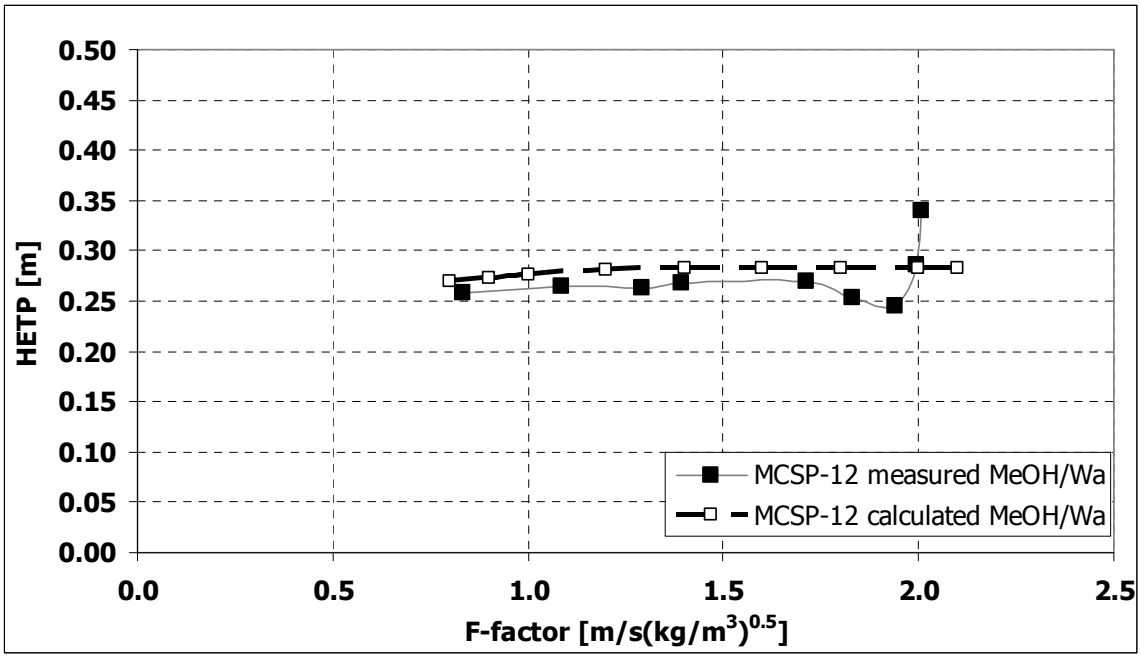

Figure 7 Measured vs. predicted HETP for MCSP-12 with methanol/water system.

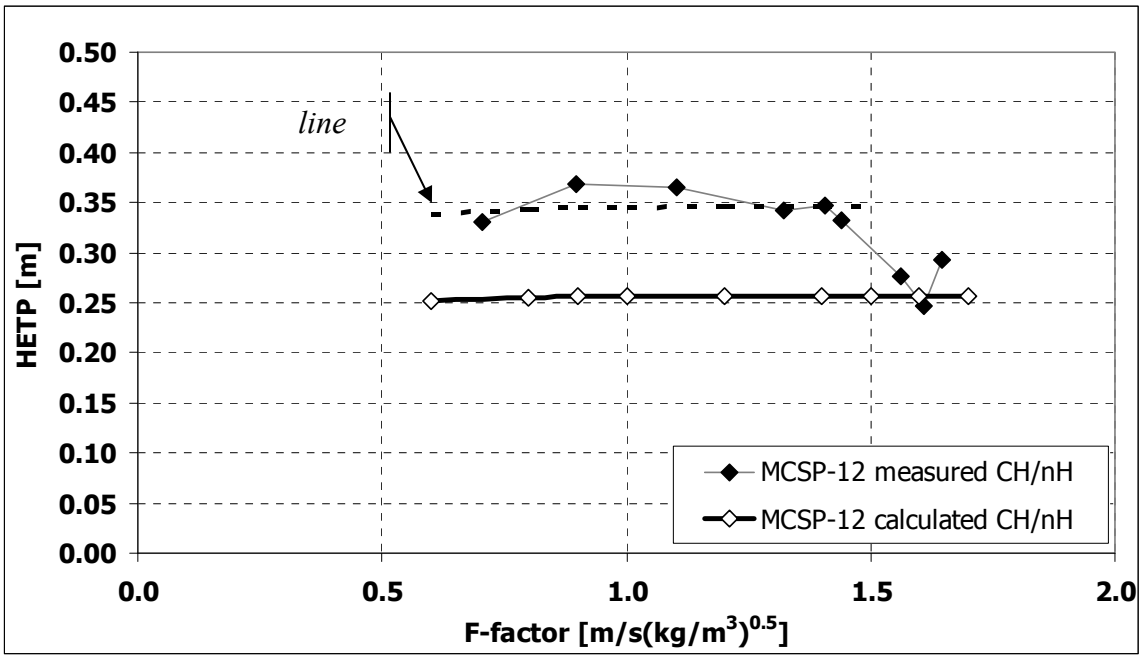

Figure 8 Measured vs. predicted HETP for MCSP-12 for the cyclohexane/n-heptane.

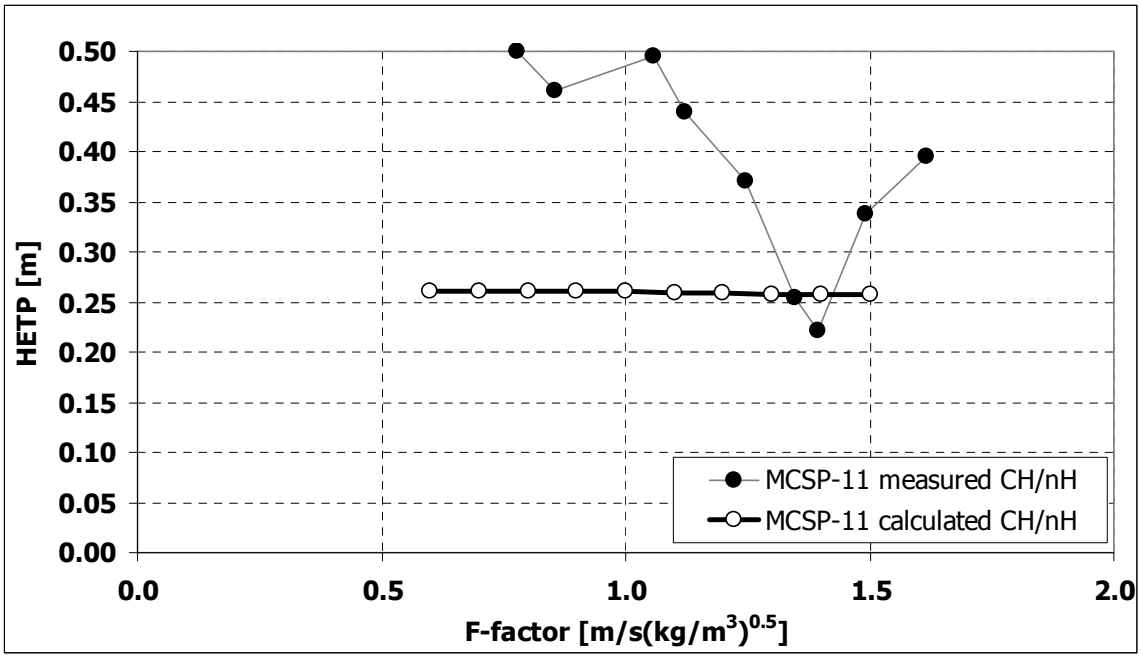

Figure 9 Measured vs. predicted HETP for MCSP-11 for the cyclohexane/n-heptane.

Table 1 Geometric features of modular catalytic structured packings (MCSP) and the high capacity structured packing (HCP) tested.

PROPERTY	SYMBOL	MCSP-12	MCSP-11	HCP
cross-sectional fraction	Γ	0.52	0.40	1
open channel ratio	X	0.5	0	1
void fraction	ε_p	0.7	0.55	0.975
specific area open channels [m^2/m^3]	$a_{p,oc}$	132.5	0	509.5
specific area closed channels [m^2/m^3]	$a_{p,cc}$	208.8	300.2	0
corrugation angle	α_c	41°		
packing element height	h_{pe}	200 mm		

Table 2 Overview of performed experiments

PACKING/SYSTEM	MEOH/WATER	C_6/C_7
HCP	X	X
MCSP-12 (Glass filling)		X
MCSP-12 (resin filling)	X	
MCSP-11		X

Table 3 Physical properties of used test systems (average at middle of the column conditions).

PROPERTY	SYMBOL	VALUE	
		MeOH/Wa	CH/nH
molecular weight [kg/kmol]	M_w	25	87
liquid density [kg/m^3]	ρ_L	854	658
dynamic liquid viscosity [Pa·s]	μ_L	$3.17\ 10^{-4}$	$2.87\ 10^{-4}$
liquid diffusivity [m^2/s]	D_L	$7.25\ 10^{-9}$	$4.35\ 10^{-9}$
surface tension [N/m]	σ_L	0.0389	0.0154
vapour density [kg/m^3]	ρ_G	1.15	3.00
dynamic vapour viscosity [Pa·s]	μ_G	$1.21\ 10^{-5}$	$8.09\ 10^{-6}$
vapour diffusivity [m^2/s]	D_G	$3.70\ 10^{-5}$	$4.53\ 10^{-6}$
liquid load at F-factor 2 [m^3/(m^{2}h)]	u_{Ls}	9.04	18.94

Table 4 Predicted catalytic liquid load points in m^3/m^{2}h and corresponding F-factors

PACKING / SYSTEM	MEOH/WA	CH/NH
MCSP-12	19.6 (F_G = 3.85)	18.6 (F_G = 1.88)
MCSP-11	-	27.5 (F_G = 2.78)